International Journal of Engineering Science 124 (2018) 16–23

Contents lists available at ScienceDirect

International Journal of Engineering Science

journal homepage: www.elsevier.com/locate/ijengsci

On the anisotropy of cracked solids

Ruslan L. Lapin[a], Vitaly A. Kuzkin[a,b,*], Mark Kachanov[c,d]

[a] Peter the Great Saint Petersburg Polytechnic University, Saint Petersburg 195251, Russia
[b] Institute for Problems in Mechanical Engineering of the Russian Academy of Sciences, Saint Petersburg 199178, Russia
[c] Department of Mechanical Engineering, Tufts University, Medford, MA 02155, USA
[d] R.E. Alexeev Nizhny Novgorod Technical University, Nizhny Novgorod 603155, Russia

ARTICLE INFO

Article history:
Received 25 October 2017
Accepted 25 November 2017

Keywords:
Effective elastic properties
Cracks
Interactions
Anisotropy
Orthotropy

ABSTRACT

We consider the effective elastic properties of cracked solids, and verify the hypothesis that the effect of crack interactions on the overall *anisotropy* – its type and orientation – is negligible (even though the effect on the overall elastic constants may be strong), provided crack centers are located randomly. This hypothesis is confirmed by computational studies on large number of 2-D crack arrays of high crack density (up to 0.8) that are realizations of several orientation distributions. Therefore, the anisotropy can be accurately determined analytically in the non-interaction approximation (NIA). Since the effective elastic properties possess the orthotropic symmetry in the NIA (for any orientation distribution of cracks, including cases when, *geometrically*, the crack orientation pattern does not have this symmetry), the orthotropy of cracked solids is not affected by interactions.

1. Introduction. The hypothesis to be verified

At low-to-moderate crack densities, the effect of crack interactions on the effective elastic properties is weak (weaker than one may expect). The reason is that, although the effect of interactions on *local* quantities such as stress intensity factors (SIFs) may be strong, the opposite effects of shielding and amplification (in arrays of cracks with random mutual positions) largely cancel one another, as directly seen from computations of Grechka and Kachanov (2006). This can also be explained by applying the internal variables technique of Rice (1975) to cracked solids: the effect of interactions on contributions of cracks to the effective properties is substantially weaker than their effect on local quantities such as SIFs (see Kachanov & Sevostianov, 2012).

Therefore, the non-interaction approximation (NIA), as applied to cracked solids, has larger-than-expected range of applicability – provided that the proper version of the NIA is used: compliances, and not stiffnesses, are linear in crack density, and the NIA is not confused with its linearized version, the "dilute limit" (see the discussion of Sevostianov & Kachanov, 2012). However, at high crack densities, the effect of interactions on the overall properties (the difference with the NIA results) becomes substantial – particularly in 2-D geometries (see, for example, computations of Kushch, Sevostianov, & Mishnaevsky, 2009 and experimental data on microcracked ceramics of Bruno & Kachanov, 2016).

The *anisotropy* of the effective properties caused by non-random orientations of cracks is another factor of importance (its knowledge may be needed, for example, for proper interpretation of various wavespeed data). The question arises, *whether the two factors – the reduction of stiffness and the anisotropy – can be separated*. We examine the hypothesis that the anisotropy can be accurately determined in the NIA, in spite of strong interactions. We assume that the anisotropy

* Corresponding author at: Peter the Great Saint Petersburg Polytechnic University, Saint Petersburg 195251, Russia.
E-mail address: kuzkin@spbstu.ru (V.A. Kuzkin).

https://doi.org/10.1016/j.ijengsci.2017.11.023
0020-7225/

is solely due to orientation distribution of cracks (crack centers do not form regular spatial patterns, such as lattice, that possess symmetries of their own).

This hypothesis is examined by computational studies of 2-D crack arrays of high crack density that have different orientation distributions. The applicability of the findings to 3-D crack geometries is discussed in the last Section of the work.

2. Background results. Anisotropy of cracked solids in the non-interaction approximation

In the NIA, the effective elastic properties of an isotropic matrix with certain distribution of cracks always possess the orthotropic symmetry – even if, *geometrically*, the orientation distribution of cracks does not have this symmetry (for example, in the case of two families of parallel cracks oriented at arbitrary angle to one another), see papers Kachanov (1980) and Kachanov (1992). The reason for this, somewhat counterintuitive, fact is that a set of 2-D non-interacting cracks can be fully characterized – from the viewpoint of the effective elastic properties – by symmetric second-rank crack density tensor (its 2-D version)

$$\boldsymbol{\alpha} = (1/A)\sum_k \left(\mathrm{a}^2 \boldsymbol{nn}\right)^{(k)} \quad in\ components,\ \alpha_{ij} = (1/A)\sum_k \left(\mathrm{a}^2 n_i n_j\right)^{(k)}, \tag{2.1}$$

where A is the area of averaging domain (2-D RVE) and $2a^{(k)}$ is the length of kth crack. Its trace $\rho \equiv \alpha_{ii} = (1/A)\sum \mathrm{a}_k^2$ is a 2-D version of the scalar crack density parameter introduced (in 3-D case) by Bristow (1960) for randomly oriented cracks; hence $\boldsymbol{\alpha}$ is a tensor generalization of ρ that accounts for crack orientations.

Indeed, the change in elastic compliances due to cracks in the 2-D case, in the NIA, is expressed in terms of $\boldsymbol{\alpha}$. The effective compliance tensor is represented as $S_{ijkl} = S^0_{ijkl} + \Delta S_{ijkl}$, where S^0_{ijkl} are compliances of the isotropic bulk material

$$S^0_{ijkl} = \frac{1+\nu'_0}{2E'_0}\left(\delta_{ik}\delta_{jl} + \delta_{il}\delta_{jk}\right) - \frac{\nu'_0}{E'_0}\,\delta_{ij}\delta_{kl} \tag{2.2}$$

and ΔS_{ijkl} are changes due to cracks

$$\Delta S_{ijkl} = \frac{\pi}{E'_0}\frac{1}{4}\left(\delta_{ik}\alpha_{jl} + \delta_{jl}\alpha_{ik} + \delta_{jk}\alpha_{il} + \delta_{il}\alpha_{jk}\right). \tag{2.3}$$

Equivalently, the result (2.3) can be expressed in terms of the change of the elastic potential due to cracks:

$$\Delta f = \left(\pi/E'_0\right)(\boldsymbol{\sigma}\cdot\boldsymbol{\sigma}){:}\boldsymbol{\alpha} = \left(\pi/E'_0\right)\sigma_{ij}\sigma_{jk}\alpha_{ik}. \tag{2.3a}$$

Hereafter, E'_0 and ν'_0 are 2-D Young's modulus and Poisson's ratio: E'_0 equals 3-D modulus E_0 for plane stress and $E_0/(1-\nu_0^2)$ for plane strain and Poisson's ratio $\nu'_0 = \nu_0$ for plane stress and $\nu'_0 = \nu_0/(1-\nu_0)$ for plane strain. In the present work, the 3-D Poisson's ratio $\nu_0 = 1/4$ will be assumed, implying $\nu'_0 = 1/3$ in the case of plane strain.

Since $\boldsymbol{\alpha}$ is symmetric second-rank tensor, the effective elastic properties are always orthotropic, the orthotropy axes being coaxial with the principal axes of $\boldsymbol{\alpha}$. We emphasize that the exact orthotropic symmetry holds only in the NIA. Indeed, for interacting cracks, tensor $\boldsymbol{\alpha}$ becomes, strictly speaking, inadequate as crack density parameter: it contains no information on mutual positions of cracks that become relevant for interacting cracks.

Remark. The same comment, that the concentration parameters that do not reflect the mutual positions of inhomogeneities, are, strictly speaking, inadequate at finite concentrations, applies to other commonly used parameters, such as scalar crack density ρ, or volume fraction, for other types of inhomogeneities. Although these parameters may distort the actual contributions of individual inhomogeneities to the effective properties, there is no simple alternative (short of solving the interaction problem). Referring to Kachanov and Sevostianov (2005) for further discussion, we focus here on the specific issue of *anisotropy* – whether it can be predicted by tensor $\boldsymbol{\alpha}$.

We examine the issue of the orthotropic symmetry for *interacting* cracks. Deviations from the orthotropic symmetry will be measured by the dimensionless Euclidean norm

$$\delta = \left\|\boldsymbol{S}^{ortho} - \boldsymbol{S}^{actual}\right\| \Big/ \left\|\boldsymbol{S}^{actual}\right\| = \sqrt{\left(S^{ortho}_{ijkl} - S^{actual}_{ijkl}\right)\left(S^{ortho}_{ijkl} - S^{actual}_{ijkl}\right)} \Big/ \sqrt{S^{actual}_{ijkl}S^{actual}_{ijkl}}, \tag{2.5}$$

where $\boldsymbol{S}^{ortho}$ is the "best-fit" orthotropic compliance tensor.

The concept of approximate and best-fit elastic symmetries was introduced by Fedorov (1968) where the best-fit isotropic approximation of elastic anisotropies was given. It was further developed, in the context of geophysics applications, by Arts, Rasolofosaon, and Zinsner (1996). For a systematic treatment of the concept and further results, see Sevostianov and Kachanov (2008); they found, in particular, that the best-fit orthotropic approximation of a given non-orthotropic tensor S_{ijkl} is given simply by setting the non-orthotropic compliances (such as S_{1112}, S_{2212}) in the axes of the best-fit orthotropy equal to zero.

Remark. In the 3-D case (circular cracks of radii a_k) – that is not considered here – crack density tensor $\boldsymbol{\alpha} = (1/V)\sum_k (\mathrm{a}^3\boldsymbol{nn})^{(k)}$ has to be supplemented by fourth-rank tensor $\boldsymbol{\beta} = (1/V)\sum_k (\mathrm{a}^3\boldsymbol{nnnn})^{(k)}$ that, however, plays a secondary role (it enters ΔS_{ijkl} with multiplier $\nu_0/2$ that is substantially smaller than the overall coefficient of 1 at the $\boldsymbol{\alpha}$-terms):

$$\Delta S_{ijkl} = \frac{32\left(1-\nu_0^2\right)}{3(2-\nu_0)E_0}\left[\frac{1}{4}\left(\delta_{ik}\alpha_{jl} + \delta_{jl}\alpha_{ik} + \delta_{jk}\alpha_{il} + \delta_{il}\alpha_{jk}\right) - \frac{\nu_0}{2}\beta_{ijkl}\right]. \tag{2.6}$$

Table 1
Parameters of crack arrays.

Number of cracks in one array	300–350
Number of boundary elements per one crack	20
Number of boundary elements per one side of the computational domain	40
Number of arrays for each crack density	450–650

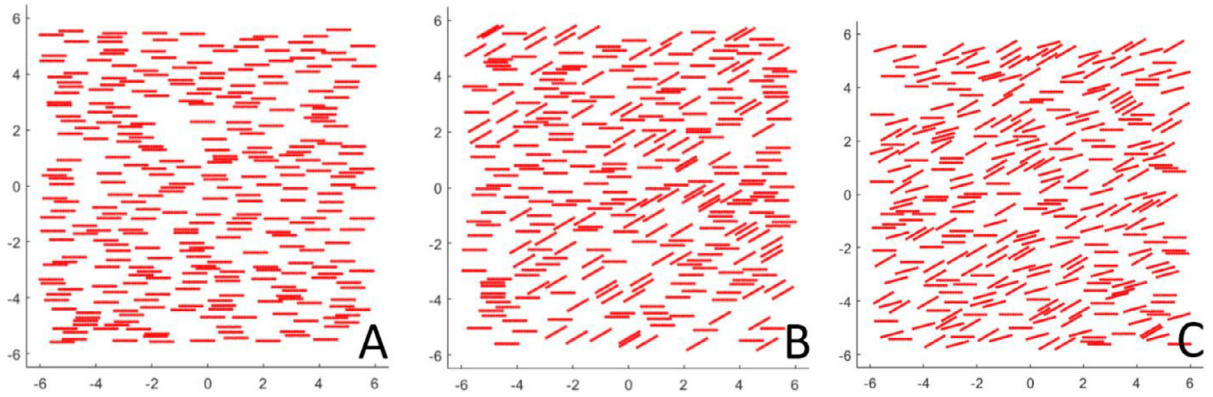

Fig. 1. Examples of the crack arrays examined. (A) Parallel crack array, (B) two families of parallel cracks, and (C) three families of parallel cracks forming angles 15° and 30° with one another. Crack density in all arrays $\rho = 0.5$.

Hence the orthotropy is approximate, even in the NIA, the deviations being due to the $\boldsymbol{\beta}$-term in (2.6) (they are actually smaller than indicated by multiplier $v_0/2$ since the $\boldsymbol{\beta}$-term contributes, partly, to the orthotropic part of the effective compliances).

3. Numerical simulations

A large number of crack arrays have been generated. The arrays were realizations of three orientation distributions:

(A) Parallel cracks;
(B) Two families of parallel cracks forming three different angles with one another;
(C) Three families of parallel cracks forming angles 15° and 30° with one another.

Note that arrays (B) and (C) do not have the *geometric* orthotropic symmetry of the orientation distribution, hence the examination of their *elastic* orthotropy is particularly important.

For all generated arrays, crack densities varied in the interval $0.01 \le \rho \le 0.8$. For each value of crack density, 450 to 650 crack arrays, each containing 300–350 cracks, were generated, with locations of crack centers determined by random number generator and subjected to the restriction of the minimal distance between cracks being larger than 0.1 crack length. This number of cracks in each array was not sufficient for the results to converge to true values of the effective compliances (as reflected in fluctuations of the results from one crack array to another). However, this factor was compensated by averaging the results over a large number of tested arrays (450–650) – the procedure that was shown to be legitimate in works of Huet and co-authors (see Hazanov & Huet, 1995; Hazanov and Amieur, 1995; Huet, 1990). Note that averaging over realizations is also widely used in molecular dynamics simulations (see e.g. paper by Kuzkin, Krivtsov, Podolskaya, & Kachanov, 2016).

In order to reduce the number of parameters involved, all cracks in the generated crack arrays had the same length. Crack centers were randomly distributed in a square computational domain, subjected to the restriction that spacing between cracks and distances between cracks and sides of computational domain were not overly small (so that the method of computation remains reliable). The minimal distance between cracks (distances between any pair of points of a given pair of cracks) or between a crack and a side of the computational domain was 0.1 of the crack length. Cracks were introduced in increments; in each increment, coordinates and orientation of a new crack were generated using a random number generator. If the newly introduced crack was overly close to the previously introduced ones or to a side of the computational domain, it was discarded and the attempt was repeated. Cracks were added until the desired crack density was reached.

To operate with dimensionless quantities, we normalize effective compliances by the shear modulus of matrix and the size of the computational domain – by crack length. Details of the numerical experiments are given in Table 1.

Fig. 1 shows examples of the crack arrays examined, for each of the three orientation distributions, (A)–(C).

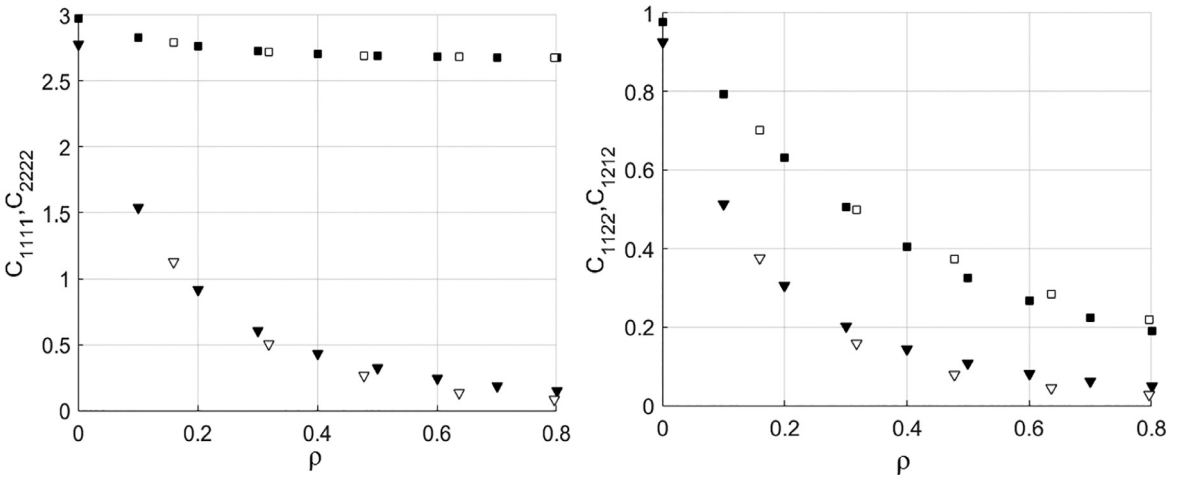

Fig. 2. Effective stiffnesses of a material with parallel cracks: comparison of our computations (black squares and triangles) with the ones of Kushch et al. (2009) (white squares and triangles).

The extra strain due to cracks $\Delta\varepsilon_{ij}$ can be expressed in terms of the average displacement discontinuities on cracks, $\boldsymbol{b}^{(k)} = \langle \boldsymbol{u}^+ - \boldsymbol{u}^- \rangle^{(k)}$, as follows:

$$\Delta\varepsilon_{ij} = \frac{1}{2A}\sum_k \left(b_i n_j + b_j n_i\right)^{(k)}, \tag{3.1}$$

where $\boldsymbol{n}^{(k)}$ is a unit normal to kth crack, A is the area of the computational domain. To compute vectors $\boldsymbol{b}^{(k)}$ for interacting cracks, we used the displacement discontinuity method (see Crouch & Starfield, 1984) that is a special case of the boundary element method (see, for example, Linkov, 2002 and the Appendix A).

To determine nine components of the (generally non-orthotropic) 2-D effective compliance tensor S_{ijkl}, we applied three test loadings:

- Uniaxial load in the "horizontal" direction ($\boldsymbol{\sigma}^0 = \sigma^0 \boldsymbol{e}_1\boldsymbol{e}_1$) so that three compliances can be determined:

$$\begin{pmatrix} S_{1111} \\ S_{2211} \\ S_{1211} \end{pmatrix} = \frac{1}{\sigma^0}\begin{pmatrix} \varepsilon_{11} \\ \varepsilon_{22} \\ \varepsilon_{12} \end{pmatrix} \tag{3.2}$$

- Uniaxial load in the "vertical" direction ($\boldsymbol{\sigma}^0 = \sigma^0 \boldsymbol{e}_2\boldsymbol{e}_2$) so that

$$\begin{pmatrix} S_{1122} \\ S_{2222} \\ S_{1222} \end{pmatrix} = \frac{1}{\sigma^0}\begin{pmatrix} \varepsilon_{11} \\ \varepsilon_{22} \\ \varepsilon_{12} \end{pmatrix} \tag{3.3}$$

- Shear load ($\boldsymbol{\sigma}^0 = \sigma^0(\boldsymbol{e}_1\boldsymbol{e}_2 + \boldsymbol{e}_2\boldsymbol{e}_1)$) so that

$$\begin{pmatrix} S_{1112} \\ S_{2212} \\ S_{1212} \end{pmatrix} = \frac{1}{\sigma^0}\begin{pmatrix} \varepsilon_{11} \\ \varepsilon_{22} \\ \varepsilon_{12} \end{pmatrix} \tag{3.4}$$

Corresponding tractions were applied at boundaries of the computational domain.

For each crack array, the effective elastic constants were computed as follows. Cracks and boundaries of the computational domain were divided into boundary elements. The system of linear algebraic equations for displacement discontinuities in all boundary elements was solved under test loading conditions mentioned above. The extra strains due to cracks were calculated according to formula (3.1) and the effective compliances – according to formulas (3.2)–(3.4).

The accuracy of the employed numerical method was examined by comparing the averaged components of the stiffness tensor for a material with parallel cracks with the results obtained by Kushch et al. (2009) by an entirely different method. The comparison shows good agreement, as seen from Fig. 2.

4. Results

Computations for the three orientation distributions of cracks, (A)–(C), produced the following results.

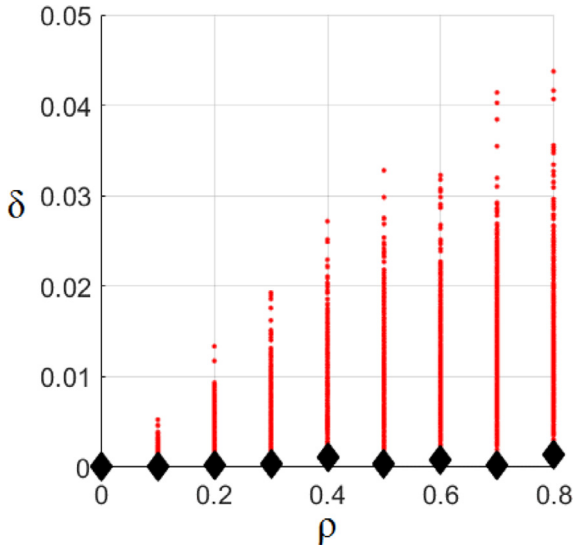

Fig. 3. Parallel cracks. Deviations from orthotropy measured by norm (2.5) at different crack densities. Vertical bars indicate the range of the deviations and diamonds – deviations of the averages (over the arrays).

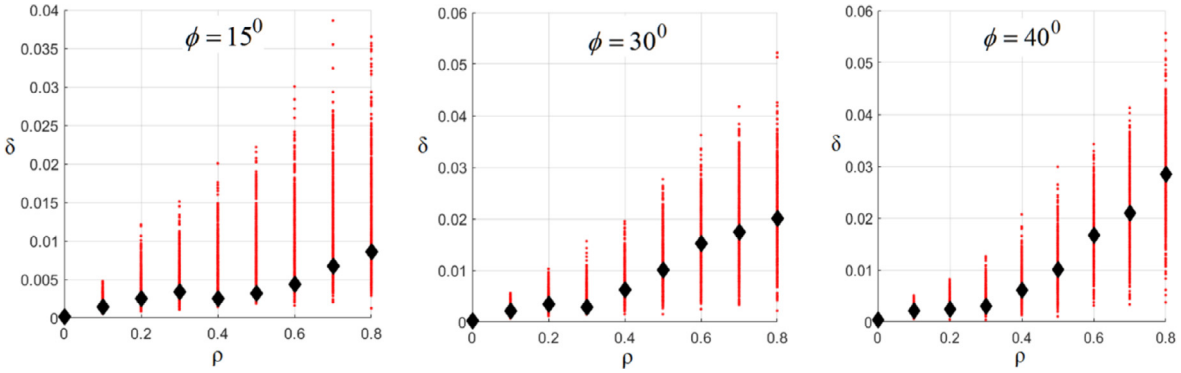

Fig. 4. Two families of cracks inclined at angle ϕ to one another. Deviations from orthotropy measured by norm (2.5). Vertical bars indicate results for specific arrays and diamonds – averages over the arrays.

(A) Parallel cracks

The deviations from orthotropy at different crack densities, as measured by the norm (2.5), are shown in Fig. 3. Note that the scatter – that is due to a finite number of cracks in an array – increases with increasing crack density. The deviation of the average, over arrays, compliance tensor from the orthotropic one (marked by diamonds) is negligible. For each of the arrays, the deviations are smaller than 4.5%.

(B) Two families of parallel cracks (inclined at angle ϕ to one another)

Partial crack densities of the two families differed by the factor of two: $\rho_1 = 2\rho_2$, $\rho_1 + \rho_2 \equiv \rho$; the overall crack density varied from 0.01 to 0.8. The orientation of the principal axes of crack density tensor $\boldsymbol{\alpha}$ is given by

$$\tan(2\gamma_*) = \frac{\rho_2 \sin(2\phi)}{\rho_1 + \rho_2 \cos(2\phi)}, \tag{4.1}$$

where γ_* is the angle between the horizontal line and one of the principal axes, counted counterclockwise. We have examined the cases $\phi = 15^\circ$, $\phi = 30^\circ$, and $\phi = 40^\circ$so that $\gamma_* \approx 4.95^\circ$, $\gamma_* \approx 9.55^\circ$, and $\gamma_* \approx 12.19^\circ$ respectively.

Deviations from orthotropy at different crack densities, as measured by the norm (2.5), are shown in Fig. 4. The deviation of the average, over arrays, compliance tensor from the orthotropic one (marked by diamonds) is within 3%. For each of the arrays, the deviations are smaller than 6%.

As far as the *orientation* of the principal axes of the "best fit" orthotropy (the concept mentioned in Section 2) of the computed compliances is concerned, Fig. 5 shows that this orientation is very accurately predicted by the NIA, i.e. by the principal axes of tensor $\boldsymbol{\alpha}$.

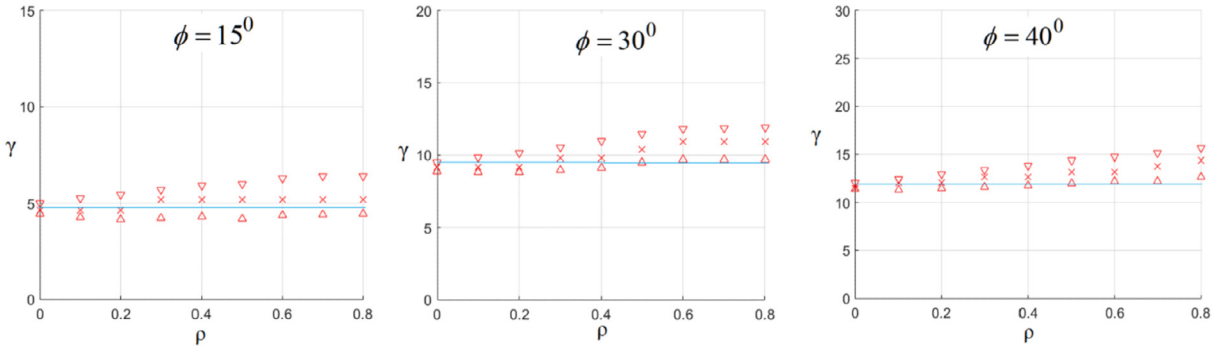

Fig. 5. Two families of cracks inclined at angle ϕ to one another. Orientation of the best-fit orthotropy for the computed compliances (crosses show averages over crack arrays and triangles – the maximal and the minimal values) vs. predictions of the NIA, formula (4.1) (solid line). The angle, in degrees, between the horizontal axis and one of the principal axes of orthotropy is shown.

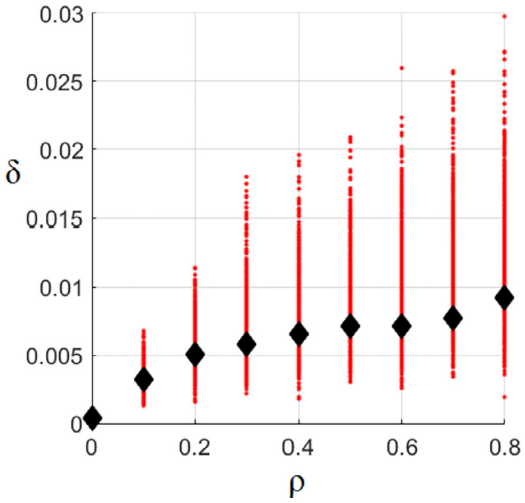

Fig. 6. Three families of parallel cracks forming angles 15° and 30° with one another. Deviations from orthotropy measured by norm (2.5). Vertical bars indicate results for specific arrays and diamonds – averages over the arrays.

(C) Three families of parallel cracks

The families form angles 15° and 30° with one another (Fig. 1c), with equal partial crack densities $\rho_1 = \rho_2 = \rho_3 (= \rho/3)$ where ρ is the overall crack density.

Deviations from orthotropy at different crack densities, as measured by the norm (2.5), are shown in Fig. 6. The deviation of the average, over arrays, compliance tensor from the orthotropic one (marked by diamonds) is within 1%. For each of the arrays, the deviations are smaller than 3%.

5. Discussion and conclusions

We verified the hypothesis that the *anisotropy* due to non-random crack orientations is accurately predicted in the non-interaction approximation (NIA), i.e. the orthotropic symmetry (with principal axes of orthotropy coaxial with the principal axes of the crack density tensor) holds – up to high values of crack densities (at which the values of the effective constants are significantly affected by interactions). Numerical simulations were done on 2-D crack arrays of three orientation distributions and different crack densities. Importantly, two of the orientation distributions did not possess the orthotropic (rectangular) *geometric* symmetry. Large numbers of arrays (450–650) generated for each orientation distribution of cracks were aimed at compensating for the relatively low number of cracks in each array (300–350).

Two further comments should be made:

1. *Implications for approximate models of the effective elastic properties*. The fact that the effective anisotropy can be taken from the NIA and thus is known *a* priori, can be useful in formulating approximate schemes for the effective elastic properties, in cases when they are anisotropic. In the self-consistent scheme, for example, cracks are placed into the matrix possessing the effective properties; since the latter is orthotropic, one has only to know compliances of cracks

of various orientations with respect to the orthotropy axes, in order to implement the scheme (in 2-D case, results are available in closed form, see Mauge & Kachanov, 1994).

2. *On applicability of the conclusions to 3-D cases*. The reported calculations were done on 2-D crack arrays, and the question arises on applicability of the main result (crack interactions do not affect the anisotropy) to 3-D arrays. To this end, we note that the interaction effects are generally weaker in 3-D, as compared to similar 2-D crack arrangements, at similar spacing between cracks (Kachanov, 1994). It can be expected, therefore, that the effect of interactions on the anisotropy is weaker than in 2-D cases – where this effect is absent. The orthotropy in the NIA is approximate in 3-D (see formula (2.6)), and the weakness of the interaction effects implies that one can expect that the accuracy of this approximate symmetry is not worsened by interactions. Further 3-D computational studies are needed to confirm this expectation.

Numerical simulations have been carried out using facilities of the Supercomputer Center “Polytechnic” at Peter the Great Saint Petersburg Polytechnic University.

Acknowledgment

One of the authors (M. Kachanov) was supported by grant 14.Z50.31.0036 awarded to R.E. Alexeev Nizhny Novgorod Technical University by the Department of Education and Science of the Russian Federation.

Appendix A. The displacement discontinuity method

This method, that represents a special case of the boundary element method (see e.g. Linkov (2002)), was introduced by Crouch and Starfield (1984). Boundaries of the domain of interest and cracks are divided into straight elements, each having the normal and the shear displacement discontinuities, D_y and D_x. The displacement discontinuity is constant along the element (zero order approximation). Higher order approximations and curvilinear elements are considered, for example, in paper by Rejwer, Rybarska-Rusinek, and Linkov (2014).

Each element can be subjected to the shear and normal loads T_x, T_y. The displacement discontinuities and loads form columns:

$$D = \begin{pmatrix} D_x^1 \\ D_y^1 \\ \dots \\ D_x^N \\ D_y^N \end{pmatrix}, \quad T = \begin{pmatrix} T_x^1 \\ T_y^1 \\ \dots \\ T_x^N \\ T_y^N \end{pmatrix} \tag{A.1}$$

that are interrelated by linear equations

$$\begin{aligned} T_x^i &= \sum_{j=1}^{N} A_{xx}^{ij} D_x^j + \sum_{j=1}^{N} A_{xy}^{ij} D_y^j \quad i = 1, ..N \\ T_y^i &= \sum_{j=1}^{N} A_{yx}^{ij} D_x^j + \sum_{j=1}^{N} A_{yy}^{ij} D_y^j \quad i = 1, ..N \end{aligned} \tag{A.2}$$

Here

$$\begin{aligned} A_{xx}^{ij} &= -2G(-\sin(2\theta) f_{xy} + \cos(2\theta) f_{xx} + y(\sin(2\theta) f_{xyy} - \cos(2\theta) f_{yyy})) \\ A_{xy}^{ij} &= -2Gy(\cos(2\theta) f_{xyy} + \sin(2\theta) f_{yyy}) \\ A_{yx}^{ij} &= 2G\left(2\sin^2\theta + \sin(2\theta) f_{xx} - y(\cos(2\theta) f_{xyy} + \sin(2\theta) f_{yyy})\right) \\ A_{yy}^{ij} &= -2G(f_{xx} - y(\sin(2\theta) f_{xyy} - \cos(2\theta) f_{yyy})), \end{aligned}$$

$$f = -\frac{1}{4\pi(1-\nu)}\left(y\left(\operatorname{arctg}\frac{y}{x-a} - \operatorname{arctg}\frac{y}{x+a}\right) - (x-a)\ln\sqrt{(x-a)^2+y^2} + (x+a)\ln\sqrt{(x+a)^2+y^2}\right),$$

where $2a$ is length of the boundary element; θ is the angle between elements i и j; G is the shear modulus; ν is Poisson's ratio; x, y are local coordinates of the jth element in the coordinate system of the ith element; f_{xy} stands for partial derivative of f with respect to x and y.

Thus, displacement discontinuities on cracks D, under given loads T, are found from the system of linear equations (A.2). In calculations considered above, loads are applied at elements representing boundaries of the computational domain; tractions at elements representing cracks are equal to zero.

References

Arts, R. J., Rasolofosaon, P. N. J., Zinsner, B. E., et al. (1996). Experimental and theoretical tools for characterizing anisotropy due to mechanical defects in rocks under varying pore and confining pressures. In E. Fjaer, et al. (Eds.), *Seismic anisotropy* (pp. 384–432). Tulsa, Oklahoma: Society of Exploration Geophysicists.

Bristow, J. R. (1960). Microcracks, and the static and dynamic elastic constants of annealed heavily cold-worked metals. *British Journal of Applied Physics, 11*, 81–85.

Bruno, G., & Kachanov, M. (2016). Microstructure-Property Connections for Porous Ceramics: The Possibilities Offered by Micromechanics. *Journal of the American Ceramic Society, 99*(12), 3829–3852.
Crouch, S. L., & Starfield, A. M. (1984). *Boundary element methods in solid mechanics* (p. 322). George Allen and Unwin.
Fedorov, F. I. (1968). *Theory of elastic waves in crystals*. New York: Plenum Press.
Grechka, V., & Kachanov, M. (2006). Effective elasticity of rocks with closely spaced and intersecting cracks. *Geophysics, 71*(3), D85–D91.
Hazanov, S., & Amieur, C. (1995). On overall properties of elastic heterogeneous bodies smaller than the representative volume. *International Journal of Engineering Science, 33*, 1289–1301.
Hazanov, S., & Huet, C. (1995). Order relationships for boundary conditions effect in heterogeneous bodies smaller than the representative volume. *Journal of the Mechanics and Physics of Solids, 42*, 1995–2011.
Huet, C. (1990). Application of variational concepts to size effects in elastic heterogeneous bodies. *Journal of the Mechanics and Physics of Solids, 38*, 813–841.
Kachanov, M. (1980). Continuum model of medium with cracks. *Journal of the Engineering Mechanics Division, 106*, 1039–1051 ASCE.
Kachanov, M. (1992). Effective elastic properties of cracked solids: Critical review of some basic concepts. *Applied Mechanics Reviews, 45*(8), S304–S335.
Kachanov, M. (1994). Elastic solids with many cracks and related problems. In J. Hutchinson, & T. Wu (Eds.), *Advances in applied mechanics* (pp. 256–426). Academic Press.
Kachanov, M., & Sevostianov, I. (2005). On quantitative characterization of microstructures and effective properties. *International Journal of Solids and Structures, 42*, 309–336.
Kachanov, M., & Sevostianov, I. (2012). Rice's internal variables formalism and its implications for the elastic and conductive properties of cracked materials, and for the attempts to relate strength to stiffness. *Journal of Applied Mechanics, 79*, 1–10 ASME.
Kushch, V. I., Sevostianov, I., & Mishnaevsky, L. (2009). Effect of crack orientation statistics on effective stiffness of mircocracked solid. *International Journal of Solids and Structures, 46*, 1574–1588.
Kuzkin, V. A., Krivtsov, A. M., Podolskaya, E. A., & Kachanov, M. L. (2016). Lattice with vacancies: Elastic fields and effective properties in frameworks of discrete and continuum models. *Philosophical Magazine, 96*(15), 1538–1555.
Linkov, A. M. (2002). *Boundary integral equations in elasticity theory* (p. 268). Dordrecht-Boston-London: Kluwer Academic Publishers.
Mauge, C., & Kachanov, M. (1994). Effective elastic properties of an anisotropic material with arbitrarily oriented interacting cracks. *Journal of the Mechanics and Physics of Solids, 42*, 561–584.
Rejwer, E., Rybarska-Rusinek, L., & Linkov, A. M. (2014). The complex variable fast multipole boundary element method for the analysis of strongly inhomogeneous media. *Engineering Analysis with Boundary Elements, 43*, 105–116.
Rice, J. (1975). Continuum mechanics and thermodynamics of plasticity in relation to microscale deformation mechanisms. In A. Argon (Ed.), *Constitutive equations in plasticity* (pp. 23–75). MIT Press.
Sevostianov, I., & Kachanov, M. (2008). On approximate symmetries of the elastic properties and elliptic orthotropy. *International Journal of Engineering Science, 46*, 211–223.
Sevostianov, I., & Kachanov, M. (2012). Effective elastic properties of heterogeneous materials: Proper application of the non-interaction and "dilute limit" approximations. *International Journal of Engineering Science, 58*, 124–128.